Low self-affine exponents of fracture surfaces of glass ceramics

Laurent Ponson[1,2],* Harold Auradou[1], Philippe Vié[3], and Jean-Pierre Hulin[1]

[1]*Laboratoire Fluides, Automatique et Systèmes Thermiques,*
UMR 7608, Universités Pierre et Marie Curie-Paris 6 et Paris-Sud,
Bâtiment 502, Campus Paris Sud, 91405 Orsay Cedex, France
[2]*Fracture Group, Service de Physique et Chimie des Surfaces et Interfaces,*
DSM/DRECAM/SPCSI, Bâtiment 462, CEA Saclay, F-91191 Gif sur Yvette, France
[3]*Laboratoire des matériaux et structures du génie civil,*
UMR 113, allée Képler, Marne la Vallée Cedex.
(Dated: February 6, 2008)

The geometry of post mortem rough fracture surfaces of porous glass ceramics made of sintered glass beads is shown experimentally to be self-affine with an exponent $\zeta = 0.40 \pm 0.04$ remarkably lower than the 'universal' value $\zeta = 0.8$ frequently measured for many materials. This low value of ζ is similar to that found for sandstone samples of similar micro structure and is also practically independent on the porosity ϕ in the range investigated (3 % $\leq \phi \leq$ 26 %) as well as on the bead diameter d and of the crack growth velocity. In contrast, the roughness amplitude normalized by d increases linearly with ϕ while it is still independent, within experimental error, of d and of the crack propagation velocity. An interpretation of this variation is suggested in terms of a transition from transgranular to intergranular fracture propagation with no influence, however, on the exponent ζ.

PACS numbers: 62.20.Mk, 46.50.+a, 68.35.Ct

Since the pioneering work of Mandelbrot [1], statistical mechanics has been used to describe fracture processes. A special attention has been brought to the statistical properties of the roughness of fracture surfaces which often display a scaling behavior referred to as *self-affinity*. This means that they are statistically invariant under the transformation : $\mathbf{r} \rightarrow \lambda \mathbf{r}$ and $h \rightarrow \lambda^\zeta h$; ($\mathbf{r}$ characterizes a location in the mean plane of the fracture, h is the surface elevation and ζ is the self-affine exponent [2]). Due to this invariance, the height-height correlation function $\Delta h(\Delta r) = < (h(\mathbf{r} + \mathbf{\Delta r}) - h(\mathbf{r}))^2 >_{\mathbf{r}}^{1/2}$ scales like :

$$\frac{\Delta h}{\Delta h(d)} = \left(\frac{\Delta r}{d} \right)^\zeta, \qquad (1)$$

$\mathbf{\Delta r}$ is a vector of constant orientation and of modulus Δr; d will be taken equal to the characteristic length scale of the microstructure of the material (the mean grain size for instance). As a consequence, the amplitude of the roughness may be characterized by the value of $\Delta h(d)$ (amplitudes corresponding to other Δr values can then be obtained from Eq. (1)).

Experimental studies of various fractured $3D$ materials provided similar values of roughness exponents $\zeta \simeq 0.8$ (see Ref. [3] for a review). These results supported the idea of a universal roughness exponent ζ independent on the material. However, sandstone fracture surfaces were found to be self-affine with a lower exponent close to 0.5 [4]. Explaining these discrepancies is important to understand the physical origin of their *self-affine* geometry. The objective of the present paper is to analyze these effects on an artificial material comparable to sandstone but with a microstructure that can be varied in a controlled manner.

Glass ceramics made of sintered glass beads have been selected for that purpose because, like sandstone, they are made of cemented grains. However, in contrast with natural rocks, both the characteristic size and the cohesion of the grains can be adjusted by modifying respectively the bead diameter and the sample porosity ϕ. The exponent ζ for these materials will be shown to be much lower than the "universal value" 0.8; in addition, it depends surprisingly little on the microstructure of the material, although the amplitude of the roughness varies significantly with the porosity. The influence of velocity on roughness reported by some authors [5] will also be evaluated by comparing two types of mode I fracturing processes with different crack propagation velocities.

The samples are prepared by heating a mold filled with a random packing of beads at $700°C$ during 20 to 200 minutes. Depending on the duration of the annealing, the degree of sintering varies and porosities ϕ ranging from 3 % to 26 % are obtained. Either of two sets of beads with diameters in the range $104-128$ μm and $50-65$ μm are used. In the following, the characteristic microscopic length scale d introduced in Eq. (1) is taken equal to the mean bead diameter. The open porosity is measured by saturating the sample with water and the profile of the total porosity along the sample is measured by γ-ray absorption. Porosity variations along the samples are of the order of 1 % so that ϕ is considered as constant and equal to this mean value within $\pm 1\%$. The process provides sintered glass cylinders with a 130 mm height and a 40 mm radius from which the samples used in the fracture tests are cut out.

Two mode I fracture tests have been performed. Fast fracture propagations are obtained by means of modified Brazilian fracture tests using toroidal samples (inside and outside radii : 10 mm and 40 mm respectively; height par-

allel to the axis : 30 mm). A uniaxial radial compression is applied to the torus and two symmetrical dynamical cracks propagate from the central hole toward the outer zones where the compressive forces are applied.

Quasistatic fracture propagations are realized on samples with a modified Tapered Double Cantilever Beam (TDCB) geometry : Their width and length are respectively 20 mm (perpendicular to the crack propagation) and 60 mm (parallel to it). The fracture is initiated from a straight notch (thickness 1 mm) by applying on both sides a uniaxial tension with a constant opening rate : The tapered shape of these specimens allows us to obtain a stable mode I crack growth (see Ref. [6]). The crack propagation velocity V_f, determined from the variations of the electrical resistance of a thin gold layer deposited on the side of the sample, remains close to 3 mm.s^{-1}.
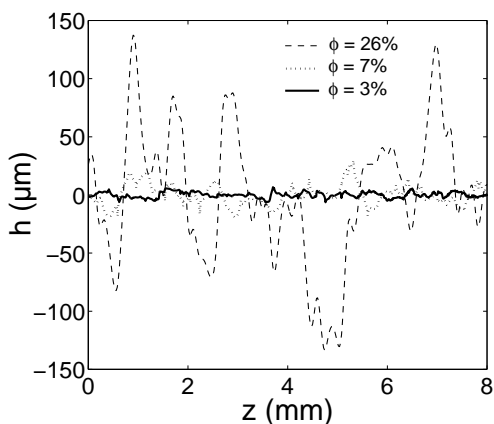

FIG. 1: Height profiles extracted from fracture surfaces of three sintered glasses with three different porosities but with beads with the same diameter $104 - 128$ μm.

Fig. 1 displays fracture surface profiles of three samples of different porosities. The roughness amplitude increases by almost two orders of magnitude from $\simeq 1$ μm for the densest ($\phi = 3$ %) to $\simeq 100$ μm for the most porous sample ($\phi = 26\%$) : Different profilometers are therefore needed to scan all the samples. For surfaces with a very low spatial roughness (and therefore porosity) we use an interferometric optical profilometer ($^{\mathrm{TM}}$Talysurf CCI 6000) with a vertical resolution better than 0.1 nm and a lateral resolution $\simeq 1$ μm. The local slope of the surface must always be small to apply this technique so that, for $\phi > 7$ %, a mechanical stylus profilometer ($^{\mathrm{TM}}$Talysurf Intra) with a $\simeq 10$ nm vertical and a $\simeq 2$ μm lateral resolutions had to be used. For lower porosities, both profilometers are usable which allowed to check the consistency of the two measurements. For both profilometers the maps contain 1024×1024 points and the fields of view are respectively 3×3 and 6×6 mm. In the second technique, the stylus is always in contact with the surface and, for porosities higher than 18%, it often gets jammed into the deepest asperities of the surface. One uses then

a point by point mechanical profilometer : A sensor tip is lowered down until it touches the surface in order to measure its height; the tip is then raised by 200 μm before getting moved laterally by 25 μm to the next measurement point. The vertical and the lateral resolutions are respectively $\simeq 3$ μm and $\simeq 10$ μm and the typical field of view is 6×6 mm. The consistency of the measurements was verified by comparing profiles provided by the two mechanical systems for $\phi = 18$ %.

These measurements provide surface elevation profiles as shown in Fig. 1. In the following, we shall only analyze profiles parallel to the z-axis (*i.e.* to the crack front) and located far enough from the initiation region so that the roughness properties are statistically stationary (this latter point is discussed in more detail below.)
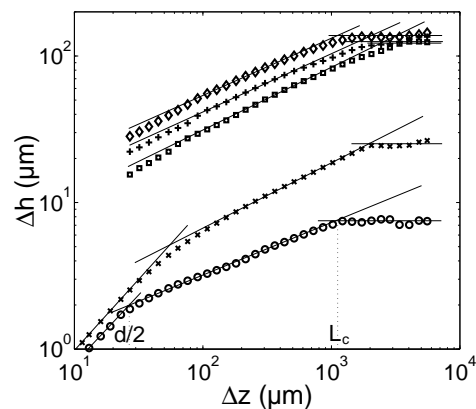

FIG. 2: Log-log representation of Δh (averaged over profiles at different x values) as a function of Δz for surface roughness profiles of several sintered glass samples. - Samples fractured using the TDCB test with porosities $\phi = 7$ % ($\times$) , 15 % ($\square$) and 26 % ($+$) - Samples fractured using the Brazilian test with porosities $\phi = 3$ % ($\circ$) and 25 % ($\diamond$) - Range of bead diameters used to realize samples : $104 - 128$ μm - Straight lines : Linear fits with slope ζ (Tab. I).

Quantitatively, these profiles will be characterized by their 1D height-height correlation function, $\Delta h(\Delta z) = < (h(z + \Delta z) - h(z))^2 >_z^{1/2}$: For surfaces with a *self-affine* roughness, the power law relationship (1) should be verified. This relation is tested in Fig. 2 which displays in a log-log scale the variations of $\Delta h(\Delta z)$ as a function of Δz for several samples : These have different porosities in the range : 3 % $\leq \phi \leq 26$ % and have been fractured both in a quasistatic mode and by the modified Brazilian test. The curve corresponds to an average of $\Delta h(\Delta z)$ over profiles corresponding to different distances x to the initiation and located in the region where the statistics of the roughness is stationary.

Let us examine, for instance, the lower curve corresponding to a 3 % porosity sample fractured using the modified Brazilian test procedure. The variation can clearly not be fitted by a single power law over the full

range of Δz values investigated : Three domains of variation are visible and correspond to exponents respectively equal to 1, 0.36 and 0 (straight lines). The last value indicates that the surface appears as a plane at large scales and the first one corresponds to an Euclidian geometry of individual grains. The surface profile is therefore self-affine (here with an exponent $\zeta = 0.36$) only in the intermediate domain between two limiting length scales : In the log-log plot of Fig. 2, they correspond to the intersections between the straight lines fitted in the different domains. The lower boundary is of the order of the bead radius $d/2$ and the upper one will be referred to as L_c.

This result is generalized by comparing the different curves in Fig. 2 corresponding to samples of different porosities and fractured both in the quasistatic and fast propagation modes. All the curves have the same global shape and, in log-log coordinates, the slopes are nearly the same in the intermediate domain : This shows that the roughness exponent is very similar in all cases while the vertical shift between the curves reflects different roughness amplitudes.

	$\phi = 3\%$	$\phi = 7\%$	$\phi = 15\%$	$\phi = 18\%$	$\phi = 25\%$	$\phi = 26\%$
	B.D.1	B.D.1	B.D.1	B.D.2	B.D.1	B.D.1
	Dyn.	*Q.S.*	*Q.S.*	*Dyn.*	*Dyn.*	*Q.S.*
Met.	$1-2$	2	3	$2-3$	3	3
ζ	0.36	0.43	0.43	0.40	0.40	0.39
ζ_{FT}	0.38	0.44	0.38	0.37	0.39	0.39
$\Delta h(d)$	3.8	8.8	32	16	56	44
L_c	1.1	1.9	2.4	0.8	1.1	1.6

TABLE I: Physical and statistical characteristics of the samples - (ϕ) sample porosity; glass beads diameter range (B.D.1) $104 - 128$ μm, (B.D.2) $50 - 65$ μm; crack propagation mode (*Dyn.*) dynamic, (*Q.S.*) quasi static; surface measurement technique (1) interferometric, (2) stylus profilometer (3) point by point - Statistical characteristic parameters of 1D profiles normal to crack propagation (ζ, ζ_{FT}) self-affine exponent values obtained respectively from the variation of Δh with Δz and from the Fourier power spectrum; ($\Delta h(d)$) roughness amplitude in μm; (L_c) upper boundary of self-affine domain in mm.

The numerical values of the parameters characterizing all these curves are listed in Table I for all samples investigated in the present work. Table I confirms that ζ has a very similar value $\zeta = 0.40 \pm 0.04$ for all samples independent of the bead size, of the porosity and of the crack propagation velocity: This common value is much lower that the value 0.8 reported for many materials and closer to the value 0.5 obtained for sandstone. This result is robust with respect to the method used to determine ζ as shown by the comparison with the values ζ_{FT} in Table I obtained from the analysis of power spectra [2]. The upper boundary L_c of the self-affine domain is of the order of $1 - 2$ mm i.e. about a tenth of the sample width and seems to decrease for faster fracture propagations. A

similar limitation of the self-affine range of length scales by finite size effects has recently been reported [7] in experiments on mortar samples of different widths.
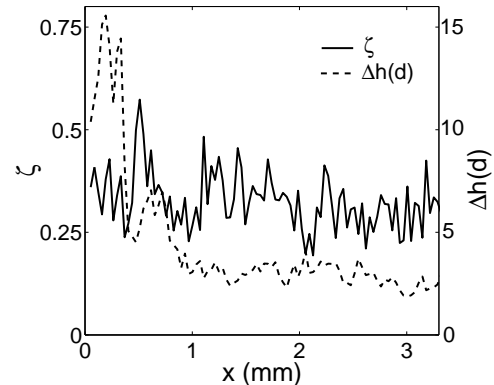

FIG. 3: Variations of the roughness characteristic exponent ζ and amplitude $\Delta h(d)$ with the distance x to the initiation notch for the same sample ($\phi = 3\%$) as in Fig.2.

In the above interpretations, it is assumed that, after a large enough propagation distance from the initiation, the statistical properties of the roughness become constant. In order to verify this assumption, the transient regime already reported by other authors [8, 9] is studied in Fig. 3. In this figure, data points correspond to single profiles parallel to z at a given distance x from the initial notch. The roughness of each profiles is characterized by its amplitude $\Delta h(d, x)$ and by the exponent $\zeta(x)$. For $x < 1$ mm, a transient regime in which $\Delta h(d, x)$ decreases with the distance x while $\zeta(x)$ remains constant is indeed observed. At larger distances, $\zeta(x)$ and $\Delta h(d, x)$ merely fluctuate around an average value. For the other samples investigated, the distance has the same order of magnitude. These results allow to restrict (as above) the statistical analysis to distances > 1 mm where the roughness is statistically stationary : This justifies our use in Fig. 2 of curves obtained from averages over several profiles corresponding to different x values.

The curves of Fig. 3 have confirmed the extreme robustness of the exponent ζ which remains constant even in the transient regime. In contrast, the roughness amplitude $\Delta h(d)$ appears to be more sensitive, not only to x, but also to the characteristic parameters of the sample like its porosity as seen in Fig. 1. This variation is analyzed quantitatively in Fig. 4, in which the normalized variable $\Delta h(d)/d$ is plotted as a function of the porosity ϕ. For low porosities, $\Delta h(d)/d$ decreases to zero while it is close to 0.5 for the most porous sample and a good collapse of all data on a linear variation is observed. This suggests that the velocity V_f of the crack propagation has a weak influence on the amplitude $\Delta h(d)$ of the roughness and that $\Delta h(d)$ is roughly proportional both to the bead size d and to ϕ.

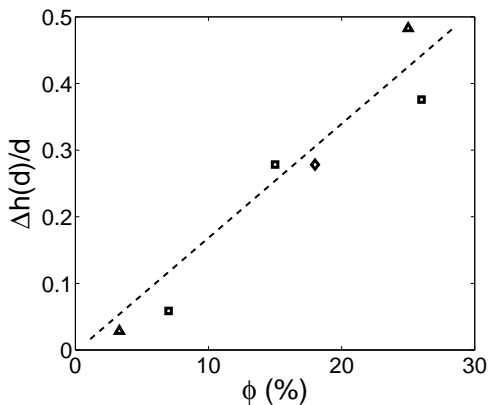These results and, particularly, the increase of $\Delta h(d)/d$

FIG. 4: Variation of $\Delta h(d)/d$ as a function of porosity ϕ. - Range of bead diameters used to realize samples -$104-128\ \mu$m ($\triangle$) : Dynamic fracture ($\square$) : Quasistatic fracture - $50-65\ \mu$m ($\diamond$) dynamic fracture. The slope of the dashed line is 1.7.

with ϕ may be related to phenomena at the scale of a bead diameter. For high porosity samples, cracks propagate by breaking cemented necks binding two beads : The difference in height between neighboring beads is then of the order of their radius and $\Delta h(d)/d \simeq 0.5$. For low porosity samples, neighboring beads are more strongly welded to each other and cracks propagate through the beads : The deflections of the surface are weaker compared to the bead radius and $\Delta h(d)/d$ is lower. This is consistent with the increase of $\Delta h(d)/d$ with ϕ in Fig. 4. These differences in the propagation of the cracks are confirmed by scanning electron microscope (SEM) images of fractured samples : These display a transition from transgranular to intergranular propagation as the porosity increases. It is remarkable that this transition has no influence on the characteristic exponent ζ.

To conclude, the fracture surfaces of sintered glass samples analyzed in the present work all display a self-affine domain of length scales characterized by an exponent $\zeta = 0.40 \pm 0.04$: This value of ζ has been found to be independent of the porosity ϕ, of the fracture propagation velocity V_f and of the diameter d of the beads. ζ is significantly lower than for many materials ($\zeta \simeq 0.8$) but close to the value found for sandstone ($\zeta \simeq 0.5$) which has a similar structure. This nearly constant value of ζ contrasts with the linear increase with ϕ of the normalized roughness amplitude $\Delta h(d)/d$ (although it is independent both of V_f and d). This increase of the amplitude likely reflects a progressive transition from transgranular to intergranular fracture propagation also demonstrated by SEM observations : A surprising feature is the fact that this transition does not influence ζ. Another important issue is the anisotropy of the surface roughness : Preliminary measurements of profiles parallel to the fracture propagation have given a value $\zeta \simeq 0.5$ larger than that reported above for profiles parallel to the front. Similar differences have been reported [10, 11] on other materi-

als using a 2D analysis based on the computation of a 2D correlation function : Applying this latter technique to the present samples might help confirm the presence and amplitude of the anisotropy. These results may be compared to the theoretical predictions of brittle fracture models describing crack growth as the propagation of an elastic line in random heterogeneous media [12, 13, 14], leading to $\zeta = 0.39$ in the 2D case [15, 16] and the 3D case [14]. Ductile fracture models such as those developed in [17] and leading to higher roughness exponent values fail to reproduce the observations reported here because damage processes are not expected during the failure of glass ceramics. Further studies are currently in progress to confirm that these models are applicable to such materials as glass ceramics or sandstone displaying brittle fracture and whether the higher value $\zeta = 0.8$ measured for many others may be associated to ductile fracture.

* Electronic address: laurent.r.ponson@wanadoo.fr
[1] B. B. Mandelbrot, D. E. Passoja, and A. J. Paullay, Nature **308**, 721 (1984).
[2] J. Feder, *Fractals* (Plenum Press, 1988).
[3] E. Bouchaud, J. Phys. Cond. Matter **9**, 4319 (1997).
[4] J. M. Boffa, C. Allain, and J. P. Hulin, Eur. Phys. J. **2**, 281 (1998).
[5] P. Daguier, B. Nghiem, E. Bouchaud, and F. Creuzet, Phys. Rev. Lett. **78**, 1062 (1997).
[6] H. Liebowitz, ed., *Fracture*, vol. 5 (Academic, 1969).
[7] G. Mourot, S. Morel, E. Bouchaud, and G. Valentin, Int. J. Frac. (*in press*) (2006).
[8] J. Schmittbuhl, S. Roux, and Y. Berthaud, Europhys. lett. **28**, 585 (1994).
[9] S. Morel, J. Schmittbuhl, J. M. Lopez, and G. Valentin, Phys. Rev. E **58**, 6999 (1998).
[10] L. Ponson, D. Bonamy, and E. Bouchaud, Phys. Rev. Lett. **96**, 035506 (2006).
[11] L. Ponson, D. Bonamy, H. Auradou, E. Bouchaud, G. Mourot, S. Morel, E. Bouchaud, C. Guillot, and J. Hulin, Int. J. Frac. (*in press*) (2006).
[12] J. P. Bouchaud, E. Bouchaud, G. Lapasset, and J. Planés, Phys. Rev. Lett. **71**, 2240 (1993).
[13] S. Ramanathan, D. Ertas, and D. S. Fisher, Phys. Rev. Lett. **79**, 873 (1997).
[14] D. Bonamy, L. Ponson, S. Prades, E. Bouchaud, and C. Guillot, Phys. Rev. Lett. (*in press*) (2006).
[15] J. Schmittbuhl, S. Roux, J. P. Vilotte, and K. J. Måløy, Phys. Rev. Lett. **74**, 1787 (1995).
[16] A. Rosso and W. Krauth, Phys. Rev. E **65**, 25101 (2002).
[17] A. Hansen and J. Schmittbuhl, Phys. Rev. Lett. **90**, 45504 (2003).